Indirect Association of Ezrin with F-Actin: Isoform Specificity and Calcium Sensitivity

Charles B. Shuster and Ira M. Herman

Programs in Cell, Molecular, and Developmental Biology and Cellular and Molecular Physiology, Tufts University Health Science Schools, Boston, Massachusetts 02111

Abstract. Whereas it has been demonstrated that muscle and nonmuscle isoactins are segregated into distinct cytoplasmic domains, the mechanism regulating subcellular sorting is unknown (Herman, 1993a). To reveal whether isoform-specific actin-binding proteins function to coordinate these events, cell extracts derived from motile (E_m) versus stationary (E_s) cytoplasm were selectively and sequentially fractionated over filamentous isoactin affinity columns prior to elution with a KCl step gradient. A polypeptide of interest, which binds specifically to β-actin filament columns, but not to muscle actin columns has been conclusively identified as the ERM family member, ezrin. We studied ezrin-β interactions in vitro by passing extracts (E_m) over isoactin affinity matrices in the presence of Ca^{2+}-containing versus Ca^{2+}-free buffers, with or without cytochalasin D. Ezrin binds and can be released from β-actin Sepharose-4B in the presence of Mg^{2+}/EGTA and 100 mM NaCl (at 4°C and room temperature), but not when affinity fractionation of E_m is carried out in the presence of 0.2 mM $CaCl_2$ or 2 μM cytochalasin D. N-acetyl-(leucyl)$_2$-norleucinal and E64, two specific inhibitors of the calcium-activated protease, calpain I, protect ezrin binding to β actin in the presence of calcium. Moreover, biochemical analysis of endothelial lysates reveals that a calpain I cleavage product of ezrin emerges when cell locomotion is stimulated in response to monolayer injury. Immunofluorescence analysis of leading lamellae reveals that anti-ezrin and anti-β-actin IgGs can be simultaneously co-localized, extending the results of isoactin affinity fractionation of E_m-derived extracts and suggesting that ezrin and β-actin interact in vivo. To test the hypothesis that ezrin binds directly to β-actin, we performed three sets of studies under a wide range of physiological conditions (pH 7.0–8.5) using purified pericyte ezrin and either α- or β-actin. These included co-sedimentation, isoactin affinity fractionation, and co-immunoprecipitation. Results of these experiments reveal that purified ezrin does not directly bind to β-actin filaments, either in solution or while isoactins are covalently cross-linked to Sepharose-4B. This is in contrast to our finding that ezrin and β-actin could be co-immunoprecipitated or co-sedimented from E_m-derived cell lysates. To explore whether calcium transients occur in cellular domains enriched in ezrin and β-actin, we mapped cellular free calcium in endothelial monolayers crawling in response to injury. Confocal imaging of fluo-3 fluorescence followed by simultaneous double antibody staining reveals a transient rise of free calcium within ezrin-β-actin-enriched domains in the majority of motile cells bordering the wound edge. These results support the notion that calcium and calpain I modulate ezrin and β-actin interactions during forward protrusion formation.

R ECENT studies indicate that the contractile protein isoforms play distinct roles in facilitating cell function. For the isoactins, there is an emerging literature to indicate that this is, indeed, the case (Rubenstein, 1990; Herman, 1993a). Three lines of evidence currently exist. First, localization studies using isoform-specific antibodies reveal that in cells simultaneously expressing muscle and nonmuscle isoactins (e.g., myocytes, smooth muscle cells, and pericytes), α-(muscle) isoactins are largely restricted to sarcomeres and stress fibers (Lubit and Schwartz, 1980; Herman, 1993b; Herman and D'Amore, 1985; DeNofrio et al., 1989; Otey et al., 1988). In contrast, β- (nonmuscle) actin is positioned in cytoplasm that is actively being remodeled, such as the membrane ruffles and forward protrusions (Hoock et al., 1991; Herman, 1993a; Hill et al., 1994). Second, over-expression of β- versus γ-nonmuscle isoactins in C2 myoblasts results in differential effects on cell surface area and morphology, respectively (Schevzov et al., 1992). And lastly, cultured cell lines expressing variants of β-actin display such phenotypes as cytochalasin resistance, altered

morphology, and heightened tumorigenicity (Ohmori, 1992; Leavitt et al., 1987; Leavitt and Bushar, 1982). These observations point to functionally diverse roles for the conventional actin isoforms and raise questions about the manner in which their subcellular segregation is achieved.

Does mRNA targeting explain the non-random distributions of isoactins observed in living cells? Pioneering studies demonstrated an association of mRNA with the cytoskeleton, since treatment of cells with cytochalasin B or RNAase A disrupted polysome distribution (Lenk et al., 1977). More recently it has been shown that actin mRNA localization can be randomized when the cellular actin network is disrupted (Sundell and Singer, 1991). mRNA anchoring is not, however, disrupted by puromycin or cycloheximide, suggesting that nascent polypeptides do not participate in mRNA localization (Sundell and Singer, 1990, 1991). Insights into isoactin mRNA targeting have also recently emerged from in situ hybridization studies on transfected cells harboring plasmids containing reporter genes, which were linked upstream of the β-actin 3' UTR. These results reveal that a β-actin mRNA targeting "address" exists in this non-coding region and directs message localization (Kislauskis et al., 1993, 1994; Hill and Gunning, 1993). These results could help to explain the selective placement of β-actin mRNA within leading lamellae, when locomotion is initiated following injury (Hoock et al., 1991; Herman, 1993c). Yet, in spite of this documented β-actin mRNA targeting, evidence is lacking to suggest that a cortical, functionally intact translational machinery either contributes to the β-actin found in these distal cytoplasmic domains or is sufficient to sequester it within the cytoskeletal–plasma membrane interface once nascent polypeptides are produced.

Mechanisms mediating β-actin dynamics in non-erythroid cells may mirror actin organization in erythrocytes, where β-actin is the lone isoform that is expressed (Pinder and Gratzer, 1983). In erythrocytes, β-actin is found as short oligomers bound by spectrin tetramers near its filament ends (reviewed by Bennett, 1985). Protein 4.1 and ankyrin foster the formation of this two-dimensional spectrin/actin lattice and join it to the plasma membrane via their association with integral membrane proteins. In a similar fashion, homologues of protein 4.1 may act to sequester β-actin in non-erythroid cells. Could ezrin, radixin, moesin, merlin, or talin, all of which are protein 4.1 homologues of the ERM family of putative tumor suppressor proteins (Tsukita et al., 1993) help to regulate isoactin dynamics in non-erythroid cells? Clearly, ezrin has been localized within membrane ruffles and cellular projections (Bretscher, 1983, 1989; Birgbauer et al., 1989), domains that we have previously reported to be enriched in β-actin (Hoock et al., 1991; Herman, 1993c). And domain mapping studies predict that the COOH-terminal portion of ezrin may associate with the actin cytoskeleton (Algrain et al., 1993; Turenen et al., 1994). However, in spite of the "historical" co-localization of these two proteins, ezrin's role as a bona fide actin-binding protein remains controversial since the full length molecule fails to bind α-actin in vitro (Bretscher, 1983, 1991).

In light of what is known about the biochemical properties and localization of β-actin and ezrin in non-erythroid cells, we asked whether ERM family members function to spatially restrict or sequester β-actin within cortical cytoplasm. To these ends, we used isoactin affinity fractionation to identify candidate polypeptides that preferentially or exclusively bind to β- versus α-actin filaments. Application of cytoplasmic extracts derived from motile cytoplasm (E_m: membrane ruffles, pseudopods, and leading lamallae) onto isoactin affinity columns reveals a population of four to six polypeptides that preferentially associate with β-, but not α-actin filaments. Western blotting of the β-actin column elutions reveals that one of the polypeptides is ezrin. In vitro association of ezrin and β-actin occurs in the presence of physiologic salts (KCl, $MgCl_2$) and EGTA, but not in the presence of micromolar levels of free calcium or cytochalasin D. The calcium-dependent inhibition of ezrin association with β-actin can be reversed with specific inhibitors of the calcium-activated protease, calpain I, or cytochalasin D. While an in vitro association of ezrin and β-actin can be demonstrated by co-precipitation of ezrin from E_m, ezrin does not directly bind to β-actin since it can neither be co-sedimented, co-precipitated, nor retained on β-actin affinity matrices when the purified molecules are mixed together. Using confocal microscopy and the calcium-sensitive fluorescent dye, fluo-3, we document transient elevations in cytosolic-free calcium occurring in moving regions of cytoplasm where β-actin and ezrin are positioned, and where calpain I–mediated ezrin proteolysis can be demonstrated. The combined results of these biochemical experiments and localization studies suggest that calcium-activated cleavage of ezrin from β-actin could facilitate isoactin dynamics during forward protrusion formation as advancing cytoplasm is remodelled during cell motility.

Materials and Methods

Vascular Cell Culture

Bovine vascular cell cultures were established as previously published (Hermana and D'Amore, 1985). Bovine retinal endothelial cell (EC)[1] and pericyte cultures were grown in DME supplemented with 5% calf serum, L-glutamine, and antibiotics; pericytes were cultured through their second passage in DME containing 10% calf serum, L-glutamine, and antibiotics.

Antibodies

Isoform-specific polyclonal antibodies were raised against α vascular smooth muscle and nonmuscle (β) actin and affinity selected as previously described (Herman and D'Amore, 1985; Herman, 1988; Hoock et al., 1991). Mouse monoclonal anti-ezrin IgG was purchased from ICN Biomedicals (Costa Mesa, CA). Anti-ezrin IgG was a gift from Dr. Anthony Bretscher (Cornell University, Ithaca, NY; Bretscher, 1983). One series of localization studies was also performed using monoclonal anti-ezrin (13H9), provided by Dr. Frank Solomon (MIT, Boston, MA).

Purification of Actin Isoforms

Muscle Actin. Acetone powder from chicken skeletal and bovine aortic smooth muscle was prepared according to previously published procedures (Spudich and Watt, 1971; Herman and Pollard, 1979). Actin was extracted from an acetone powder in G buffer (2 mM Tris-HCl, 0.2 mM $CaCl_2$, 0.2 mM DTT, 0.2 mM ATP, 0.02% NaN_3) and cycled through one round of polymerization–depolymerization prior to gel permeation chromatography on Sephadex G-150.

Erythrocyte Actin. Erythrocyte acetone powder was prepared as previously described (Puszkin et al., 1978), with several modifications. Acetone powder was extracted twice using 15 ml G buffer/gram powder for 2 h at 4°C. After clarification at 27,000 g for 1 h at 4°C, the extract was fractionated over DEAE cellulose (DE-52; Sigma Chem. Co., St. Louis, MO)

---

1. Abbreviations used in this paper: CNBr, cyanogen bromide; DSP, dithiobis(succinimidylpropionate); EC, endothelial cells; LB, lysis buffer.

equilibrated with G buffer, and released with a linear gradient of 0.05–1.0 M NaCl. Actin eluted from the column between 0.15–0.25 M NaCl. These fractions were pooled, concentrated to 4–6 ml, and applied to a 3 cm × 48 cm Sephadex G-150 column equilibrated with G buffer. Peak actin fractions were then pooled, and filaments were assembled at room temperature in 2 mM $MgCl_2$ and 100 mM KCl. After centrifugation at 100,000 g, F-actin was disassembled in G buffer, sterile-filtered, and rechromatographed on G-150 Sephadex prior to storage on ice. SDS–gel electrophoresis as well as isoelectric focusing of purified actins demonstrate that each isoactin pool is greater than 98% pure, both at the level of isoactins and with respect to other contaminating proteins.

Preparatin of F-actin Affinity Matrices

Isoactins were covalently cross-linked to Sepharose-4B by cyanogen bromide (CNBr) activation as described (Herman and Pollard, 1979). Briefly, 20 ml Sepharose-4B was washed three times with deionized water at 4°C by pelleting/resuspension. Washed Sepharose-4B was resuspended in an equal volume of dH_2O and allowed to warm to 15°C prior to activation with CNBr (0.25 g/ml beads). The pH was held between 10.5–11.0 using 6 N NaOH for 15 min, prior to washing (2 liters, 0.1 M Sodium borate, pH 8.8). Following dialysis in borate buffer, equal volumes of phalloidin-stabilized actin (0.5 mg/ml, 11.6 μM; 1:4 molar ratio; phalloidin/actin) and washed CNBr-activated Sepharose-4B were mixed overnight at 4°C. Unbound actin was removed by pelleting and resuspension in excess borate buffer prior to quenching with 100 mM glycine, 20 mM Tris-HCl, 0.2 mM $CaCl_2$, pH 7.8, overnight at 4°C. The concentration of bound actin ranged from between 4.1 and 5.0 μM (0.17–0.22) mg/ml. Phalloidin-stabilized F-actin bound to Sepharose-4B was either used immediately or stored on ice in 20 mM Tris-HCl, pH 7.8, 70 mM KCl, 0.2 mM DTT, 0.2 mM ATP, 0.1 mM $CaCl_2$, 0.02% NaN_3.

Extraction of Retinal Pericytes for Affinity Fractionation

Subconfluent pericyte cultures were washed three times with PBS at room temperature prior to extraction for 10 min at room temperature in lysis buffer (LB) (3 ml/10^6 cells). LB contains either 0.1% Triton X-100 or 34 mM octyl-glucoside, 40 mM Hepes, pH 7.15, 50 mM Pipes, pH 6.9, 75 mM NaCl, 1 mM $MgCl_2$, 0.5 mM EGTA, 1 mM PMSF, 0.1 mg/ml pepstatin, 0.1 mg/ml SBTI, 0.1 mM TLCK, 0.1 mM TPCK, 1 mM TAME, and 2.5 mM sodium orthovanadate. Alternatively, cells were lysed in LB that contained either 0.2 mM $CaCl_2$ or 0.2 mM $CaCl_2$ with 0.1 mg/ml calpain inhibitor I (N-acetyl-[leucyl]$_2$-norleucinal; Boehringer-Mannheim Biochemicals, Indianapolis, IN) (Tsujinaka et al., 1988). In other experiments, 5 μM E64 (L-trans-epoxysuccinyl-leucylamido [4-guanidino]butane) (Sigma Chem. Co.), another inhibitor of calpain I, was used (Barrett et al., 1982). After removal of the Triton-soluble fraction, the Triton-insoluble fraction was dissolved using LB containing 0.1% SDS. Fractions were clarified at 20,000 g, and then dialyzed against three changes of G buffer containing either 0.2 mM $CaCl_2$, 0.2 mM $MgCl_2$/0.5 mM EGTA, 100 mM NaCl at either 0°C or room temperature. Protein content was determined colorimetrically (Bio-Rad-Laboratories, Richmond, CA).

Isoactin Affinity Fractionation

Lysates (Triton-soluble, 1–2 × 10^6 cells) that were dialyzed as described above were mixed for 4–20 h with muscle-actin Sepharose-4B, either at 4°C or room temperature. Unbound protein was collected, split into two equal fractions and re-applied to both α- and β-actin Sepharose-4B. Following exhaustive washing, bound proteins were eluted using a 0.1, 0.5, and 1.0 M KCl step gradient. Fractions were collected into chilled tubes, dialyzed (versus G buffer), and then lyophilized prior to boiling in SDS-PAGE sample buffer containing 10% 2-mercaptoethanol and electrophoresis on 10% SDS-PAGE mini gels. Fractions were either directly visualized by silver staining or transferred to nitrocellulose for Western blotting with anti–ezrin or –actin antibodies using previously described procedures (Herman, 1988; DeNofrio et al. 1989).

Co-immunoprecipitation of Ezrin and Actin from Lamellar Extracts

Retinal pericytes were labelled for 10 h with 85 μCi/ml [^{35}S]methionine/[^{35}S]cysteine (Translabel; ICN Biomedical), in methionine- and cysteine-deficient DME supplemented with 10% calf serum, glutamine, and

antibiotics. Media was briefly exchanged with three washes of PBS. To stabilize any low-affinity, protein–protein interactions against the detergents present in the lysis and immunoprecipitation buffers, cells were treated with the thiol-reducible, cross-linking agent dithiobis(succinimidylpropionate) (DSP) (Pierce Chem. Co., Rockford, IL) (0.25 mM) in PBS containing 0.002% Digitonin for 10 min at room temperature. Cells were washed three times with 10 mM Tris-HCl, 150 mM NaCl, pH 7.4, to quench residual DSP, prior to lysis in 0.5 ml 0.5% Triton X-100, 40 mM sodium pyrophosphate, pH 7.5, 150 mM NaCl, 1 mM EGTA, 1 mM EDTA, 2 mM DTT, 5 mM ATP, 5 mM iodoacetamide, supplemented with 0.1 mM PMSF, 0.1 mg/ml soybean trypsin inhibitor, 0.1 mg/ml pepstatin, 2.5 mM sodium orthovanadate, 0.1 mM TLCK, 0.1 mM TPCK, and 1 mM TAME (LB$_i$) for 10 min at room temperature. Immunoprecipitation was performed as previously described (Yost and Herman, 1990). To ensure loading of samples, TCA precipitation was performed on duplicate samples to determine incorporation of [^{35}S]methionine/cysteine into total cell protein, and equal counts were loaded. Samples were resolved on 7.5% SDS-PAGE and then processed for fluorography (Laskey and Mills, 1975).

Quantification of Ezrin in Cell Lysates

To quantify the amount of ezrin present in vascular cell lysates, immunoprecipitation was performed from pericyte E_m as described above (Yost and Herman, 1990). Immunoprecipitated ezrin was resolved by SDS-PAGE and transferred to Immobilon PDVF membrane (Millipore Corp., Milford, MA). After staining with 0.1% Coomassie R-250, the ezrin band (as identified by parallel Western blotting) was excised and treated with 6 N HCl for 24 h at 110°C. Amino acid analysis was then performed using PICO·TAG amino acid analysis sytem (Waters, Milford, MA) in the protein analysis facility (Department of Physiology, Tufts University, Boston, MA) (Cohen et al., 1984). The identity of the excised band was confirmed as ezrin by comparing the mole fraction of amino acids present to those predicted (Gould et al., 1989). The concentration of ezrin in pericytes was determined to be 7.7 pmol/10^6 cells.

Purification of Pericyte Ezrin

Native, intact ezrin was purified from cultured bovine retinal pericytes essentially as described (Bretscher, 1983, 1986) with the following modifications. 2.5 × 10^7 cells were lysed in 4 ml LB per 150 mm dish as described for isoactin affinity fractionation (see above). Following clarification of the ezrin-containing lysate at 27,000 g for 15 min at 4°C, it was dialyzed against three changes of 10 mM imidazole, pH 6.7, 20 mM NaCl, 1 mM DTT, and 0.1 mM PMSF at 0°C. The lysate was clarified by centrifugation at 100,000 g for 30 min, 4°C prior to application onto a 1.0 × 4.0 cm hydroxylapatite column pre-equilibrated with 100 mM KH_2PO_4, pH 7.0. Ezrin-containing fractions were eluted with a 40 ml linear gradient of KH_2PO_4 (0.1–0.8 M) containing 5 μM E64 to inhibit proteolysis. 1-ml fractions were collected and analyzed by 10% SDS-PAGE. Ezrin-containing fractions were identified by ELISA and subsequently pooled prior to dialysis against 10 mM Tris-Cl, pH 7.5, 1 mM DTT, 0.5 mM EGTA. The pooled fraction was re-clarified prior to loading onto a 0.5 × 1.0 cm column of DEAE cellulose (DE-52; Sigma Chem. Co.) equilibrated in 10 mM Tris, pH 7.5, 1 mM DTT, 0.5 mM EGTA. Fractions were eluted with a linear NaCl gradient (0–0.2 M). Ezrin elutes in the middle of the gradient (0.1 M NaCl). Ezrin purity was assessed by SDS-PAGE, and judged to be >92% pure by densitometry. Its identity was also confirmed by Western blotting (see above). Purification of ezrin by this affinity isolation procedure yielded a 1,000-fold enrichment where 15–20 μg of ezrin could be purified from 15 mg of starting material. Ezrin was stored in 10 mM Tris-Cl pH 7.5, 1 mM DTT, 20 mM NaCl, 0.5 mM EGTA, 0.02% NaN_3 on ice.

Interaction of Pericyte Ezrin with Gel-filtered Isoactins

Co-sedimentation Analysis. Gel-filtered (0.5 μM) skeletal muscle (α) and erythrocyte (β) actin were assembled separately into filaments following a second round of polymerization. Actin assembly proceeded in the barrel of a 1-cc syringe at 37°C for 30 min prior to shearing through a 25-gauge needle. This yielded many foreshortened filaments, maximizing the number of filament ends. Filament lengths prior to shearing were 3.7 ± 0.65 μm, and following shearing were 0.75 ± 0.2 μm as measured by negative stain transmission electron microscopy. 290 μl of sheared filaments were added to prewarmed microfuge tubes containing 10 μl of either F-actin buffer or 40 μg/ml ezrin. Either ezrin-containing lamellar lysates or purified ezrin was mixed with isoactin filaments by rotation for an additional 30 min at either

room temperature or 37°C. The mixtures were then pelleted by centrifugation at 110,000 g in a Beckman TLA 100.2 rotor (Beckman Instruments, Palo Alto, CA) for 35 min at 15°C. The supernatants were removed, and the proteins present in the supernatant and pellet fractions quantitatively precipitated using 3 vol of ice cold ethanol (100%). Protein pellets were dried in a Speedvac (Savant, Farmingdale, NY), and re-solubilized in boiling SDS-PAGE sample buffer. Supernatant and pellet fractions were analyzed by 10% SDS-PAGE and Western blotting (DeNofrio et al., 1989).

Immunoprecipitation of Ezrin-Actin Complexes. Twice-polymerized isoactin filaments were incubated with pericyte ezrin as described above. Anti-actin IgG-coated Affigel beads (Bio-Rad Laboratories, Richmond, CA) were prepared exactly as described (Yost and Herman, 1990). Ezrin-actin (1:300 molar ratio; ezrin/actin) mixtures were incubated with anti-actin IgG-coated affigel beads at a 4 molar excess of IgG to actin for 3 h at room temperature. Immunoprecipitates were washed three times by pelleting, and resuspension in F-actin buffer prior to boiling in SDS-PAGE sample buffer and Western blotting for ezrin using mouse monoclonal anti-ezrin IgG (ICN Biomedicals) and alkaline phosphatase-conjugated goat anti-mouse IgG (Bio-Rad Laboratories).

Isoactin Affinity Fractionation of Purified Ezrin. To further assess whether purified pericyte ezrin could bind directly to the isoactin affinity columns, 0.5 μg (~10⁶ cell equivalents) ezrin in G buffer (with 0.2 mM MgCl₂, 0.5 mM EGTA, ± 100 mM NaCl) was mixed with 0.5 ml of 5 μM (α or β) actin Sepharose-4B in a fashion identical to that described for affinity fractionation of Eₘ. Isoactin Sepharose-4B–ezrin mixtures were incubated for 3 h at room temperature, and the unbound fractions were collected. Columns were washed, and bound protein eluted with 1 M NaCl. Protein present in the unbound fractions and 1.0 M NaCl elutions were quantitively precipitated (with ethanol), and probed for the ezrin by Western blotting.

Simultaneous Localization of Ezrin and β-Actin by Double Antibody Staining

Bovine endothelial cells were plated at confluence, injured with a fire-polished pasteur pipet and allowed to recover for 60 min at 37°C, and then were fixed and processed for indirect immunofluorescence according to previously published procedures (Hoock et al., 1991). For ezrin localization, 2 μg/ml affinity-purified, rabbit anti-ezrin IgG (Bretscher, 1983) or 5 μg/ml monoclonal anti-ezrin IgG (ICN Biomedicals) were used. For anti-β-actin IgG localization, 5-50 μg/ml affinity-selected antibodies were used (Hoock et al., 1991). Cells processed for co-localization were viewed using either an Odyssey laser scanning confocal microscope (Krypton-argon laser; Noran Instruments, Middleton, WI) or a Zeiss IM 35 inverted fluorescent microscope equipped with a 50 W Hg lamp and a Zeiss planapochromat oil immersion objective lens (NA 1.4). Confocal images were stored in TIF files (Metamorph; Universal Imaging, West Chester, PA), and fluorescence micrographs were recorded with Tri-X film (Herman and D'Amore, 1985).

Localization of Free Calcium in Motile Endothelial Cells

To examine calcium transients in migrating cells, resting endothelial monolayers were injured in the presence of 5 μM Fluo-3 as described above (Molecular Probes, Eugene, OR). Coverslips with cells attached were then mounted on a warmed chamber slide and allowed to recover 30-120 min at 37°C on the confocal microscope stage. Image capture, processing and quantification was accomplished using Metamorph (Universal Imaging, West Chester, PA). Coverslips with cells attached were then processed for simultaneous anti-ezrin and anti-β-actin indirect immunofluorescence. Ezrin and β-actin images were paired and scaled using Optimas (Bioscan Incorporated, Edmonds, WA) and Adobe Photoshop (Adobe Systems Incorporated, Mountain View, CA). To record the frequency of Ca²⁺ transients in the leading lamellae of motile cells, random fields of cells bordering the wound edge were selected by transmitted light microscopy, and the incidence of Fluo-3 fluorescence was recorded for 100 cells per experiment (n = 3).

Results

Isoactin Affinity Fractionation: Identification of β-Actin–binding Proteins

Our earlier work revealed a selective, non-random distri-

bution of β-actin and its encoding mRNA within the forward protrusions of locomoting endothelial cells and fibroblasts recovering from monolayer injury (Hoock et al., 1991). Since then, we have tested whether retention of locally translated or recently transported β-actin (to the membrane-associated, cortical cytoskeleton) is dependent upon β-actin–specific binding protein(s). To this end, we prepared Sepharose-4B columns containing homogeneous populations of phalloidin-stabilized actin filaments purified from either skeletal muscle (α; chicken), vascular smooth muscle (α; bovine) or erythrocytes (β; bovine or human). Sequential fractionation of extracts derived from spreading cytoplasm (Eₘ) over these isoactin affinity matrices afforded an opportunity to identify putative α- and/or β-actin-specific binding proteins (bABPs).

Based on the solubility properties of the isoactin network present in mobile projections (DeNofrio et al., 1989; Rubenstein, 1981), we presumed that bABPs would also be present in Eₘ, associated with their respective isoactins using either 34 mM octyl-glucoside or 0.1% Triton X-100. When Eₘ (250 μg/ml) (Fig. 1, lane 1) is percolated over 5 μM α- (skeletal or smooth muscle) actin columns, 4% of the protein pool (10 μg bound/ml α-actin Sepharose-4B) is retained.
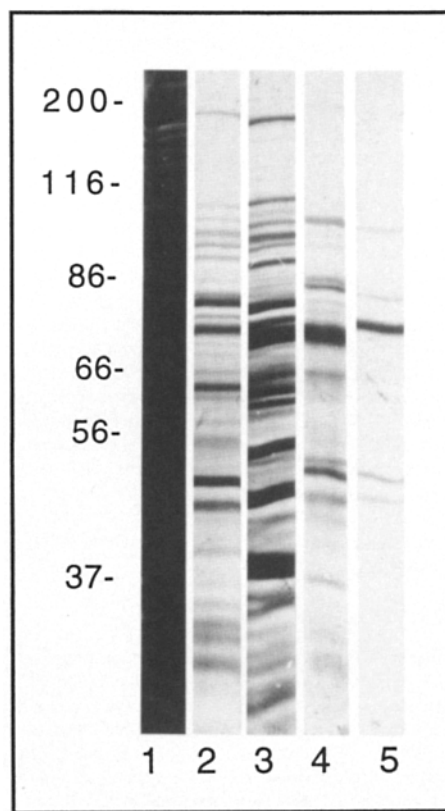

Figure 1. Affinity selection of β-actin–binding proteins. Retinal pericytes were lysed in a buffer containing 0.1% Triton X-100 (as described in Materials and Methods). Following dialysis to remove detergent, lysate (lane *1*) was applied to skeletal muscle–Sepharose-4B (α-actin). Bound proteins were eluted using 1 M KCl (lane *2*). The flow-through (lane *3*) was re-applied to erythrocyte actin–Sepharose-4B (β-actin) (in the presence of 0.2 mM MgCl₂/0.5 mM EGTA [lane *4*] or 0.2 mM CaCl₂ [lane *5*]), and bound proteins eluted with 1.0 M KCl (lanes *4* and *5*). The eluted fractions were resolved on 10% SDS-PAGE gels and visualized by silver staining.

Following exhaustive washing, bound proteins are released with 1.0 M KCl (Fig. 1, lane 2). Inclusion of 100 mM NaCl in the dialysis and affinity fractionation buffers does not alter the constellation of polypeptides eluted (data not shown). SDS–gel electrophoresis and silver staining reveals between 20–22 polypeptides present in fractions released from α-actin–Sepharose-4B. These include several in the lower (34, 37/38, 40/43, 51, 53 kD), middle (69/73, 78, 98, 100, 105/107, 118 kD), and high molecular weight ranges (200, 250 kD) (Fig. 1, lane 2). Western blotting of these polypeptides electrophoresed and transferred to nitrocellulose indicate that myosin II, fodrin (α chain), and caldesmon (low and high molecular weight isoforms) are amongst the actin-binding proteins that can be released from α skeletal and α-smooth muscle actin Sepharose-4B. While these actin-binding proteins share identical elution profiles from α- and β-actin affinity columns, dot blot overlay analysis reveals that one polypeptide, p34 calponin, preferentially binds filaments of smooth muscle actin (Shuster, C. B., I. M. Herman, manuscript in preparation).

When the flow-through fraction (Fig. 1, lane 3), which is not retained on α-actin–Sepharose-4B, is reapplied to 5 µM β-actin–Sepharose-4B, only 1.5–3% of the total E_m protein pool (4–7.5 µg bound/ml β-actin–Sepharose) is retained (Fig. 1, lane 4). Silver staining of this fraction reveals 11 polypeptides, 5 of which were present in the α-actin–binding fractions (Fig. 1, lane 2). The remaining six polypeptides preferentially bind and can be released from β-actin Sepharose-4B (Fig. 1, lane 4). These include polypeptides of 35, 65, and doublets of 70–73 and 80/83 kD. These bABPs can be released from the β-actin affinity columns using 1.0 M KCl (Fig. 1, lane 4). While inclusion of 100 mM NaCl in affinity fractionation buffers does not affect the binding of these bABPs, inclusion of 0.2 mM $CaCl_2$ reduces or obliterates the association of two polypeptides, most notably those polypeptides at 65 and 80/83 kD (Fig. 1, lane 5).

Ezrin Present within Lamellar Extracts Specifically Associates with β, but Not α-Actin Filaments: Calcium Sensitivity and Calpain Activation

Ezrin, along with other ERM family members, has been localized within the cortical cytoskeleton; but intact, native ezrin does not bind muscle actin in vitro (Bretscher, 1983, 1989; Birgbauer and Solomon, 1989). Therefore, we wished to explore whether ezrin was one of the β-actin–specific binding proteins present in the 65–85 kD elutions isolated from β-actin Sepharose-4B. After probing this E_m-derived fraction with monoclonal or polyclonal anti-ezrin IgGs, we see that ezrin does not bind parallel α-actin columns. However, ezrin present in the α-actin Sepharose-4B flow-through specifically binds and can be released from β-actin columns. With a KCl step gradient, 20% of the bound ezrin is released with 0.1 M KCl, 78% with 0.5 M, and 2% with 1.0 M KCl. Since ≥98% of the bound ezrin can be released with 0.5 M KCl, 1.0 M KCl was used for all further experiments to strip β-actin columns of associated ezrin (Fig. 2).

When E_m lysates are fractionated in the presence 0.2 mM $CaCl_2$, the immunoreactive ezrin species is barely detectable, even in the 1.0 M KCl releasates derived from either α- or β-actin affinity columns at 4°C or room temperature (Fig. 2, lanes 4 and 5; respectively; Table I). Based on densitometric analyses, there is roughly a 20-fold difference in
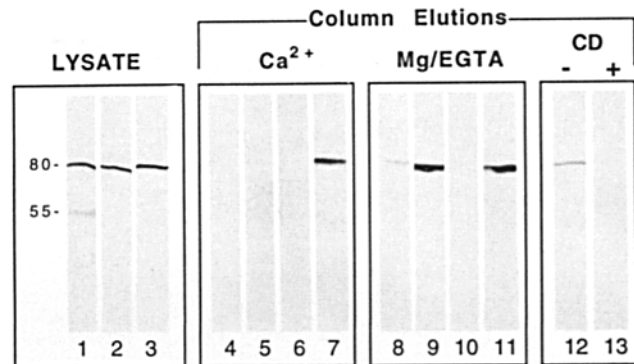

Figure 2. Calcium–calpain I regulates β-actin–ezrin interactions. Lamellar lysates were absorbed over α-actin Sepharose-4B, and the flow-through was re-applied to parallel α- and β-actin affinity columns. To test the effects of divalent cations on the association of ezrin and β-actin, extracts were prepared, and subsequent isoactin affinity fractionation was performed in the presence of 0.2 mM $CaCl_2$ (lanes 4 and 5), 0.2 mM $MgCl_2$/0.5 mM EGTA (lanes 8 and 9), or Mg^{2+}/EGTA with 100 mM NaCl (lanes 10 and 11). Further, to examine whether the interaction of ezrin and β-actin was regulated by calpain I, lysates were derived and isoactin affinity fractionation performed in buffers containing 0.2 mM $CaCl_2$, which also included 5 µM E64, a specific inhibitor of calpain I (lanes 6 and 7). Finally, to assess whether ezrin-binding to β-actin occurred via the ends of the isoactin filament or along their lengths, phalloidin-stabilized isoactin filaments covalently attached to Sepharose 4B were treated with 2 µM cytochalasin D prior to percolatin of lamellar extracts over isoactin columns (lanes 12 and 13). Proteins bound and eluted from isoactin affinity columns were resolved on 10% PAGE gels, transferred to nitrocellulose, probed with 1 µg/ml anti-ezrin IgG, and visualized with 1 µg/ml goat anti–rabbit IgG–horseradish peroxidase. (Lane 1) Lysate prepared in the presence of 0.2 mM $CaCl_2$. (Lane 2) Lysate prepared in the presence of 0.2 mM $MgCl_2$/0.5 mM EGTA. (Lane 3) Lysate prepared in the presence of 0.2 mM$CaCl_2$ with 5 µM E64. (Lane 4) α-actin–Sepharose eluted with 1 M KCl. (Lane 5) β-actin–Sepharose eluted with 1 M KCl. (Lane 6) α-actin–Sepharose eluted with 1 M KCl. (Lane 7) β-actin–Sepharose eluted with 1 M KCl. (Lane 8) α-actin–Sepharose eluted with 1 M KCl. (Lane 9) β-actin–Sepharose eluted with 1 M KCl. (Lane 10) α-actin–Sepharose eluted with 1 M KCl. (Lane 11) β-actin–Sepharose eluted with 1 M KCl. (Lane 12) β-actin–Sepharose eluted with 0.5 M KCl. (Lane 13) Cytochalasin D–pretreated β-actin–Sepharose eluted with 0.5 M KCl.

ezrin released (from β-actin columns) when affinity fractionation is performed in the presence of EGTA ($n = 7$) versus Ca^{2+} ($n = 7$) (Fig. 2, lane 9; Table I). Ezrin–β-actin interactions are maintained when calcium is chelated, and under low (G buffer) or near physiologic (100 mM NaCl) salt concentrations (Fig. 2, lane 11). Under all of these experimental conditions, ezrin binding to parallel skeletal or smooth muscle actin columns is not measurable ($n = 14$) (Fig. 2, lanes 4, 6, 8, and 10).

To learn whether the effect of calcium on the association of ezrin with β-actin is via calcium-activated proteases, E_m lysates were derived and fractionated in the presence of 0.2 mM $CaCl_2$ with or without peptide inhibitors of the neutral cysteine proteases, calpain I, and calpain II. A report in the literature has indicated that calpain I catalyzes a limited proteolysis of ezrin, yielding a major species of 55 kD (Yao et al., 1993). Indeed, western blotting reveals a 55-kD breakdown product (ezrin p55) present in E_m prepared in the presence of 0.2 mM $CaCl_2$ (Fig. 2, lane 1), which in-

Table I. Quantitative Analysis of β-actin–Ezrin Interactions

	20°C				4°C			
	β		α		β		α	
	Percent control*	Molar ratio‡	Percent control	Molar ratio	Percent control	Molar ratio	Percent control	Molar ratio
Ca²⁺	5.6	0.24	5.8	0.23	3.4	0.13	ND§	ND
Ca²⁺/E64	61	2.40	ND	ND	57	2.24	ND	ND
EGTA	100	3.94	10	0.39	59	2.34	ND	ND
EGTA/100 mM NaCl	75	2.94	ND	ND	55	2.17	ND	ND

* Percentage of ezrin released from β- and α-actin–Sepharose-4B affinity columns in the presence of EGTA. Ezrin was identified by western blotting as described in Materials and Methods. Bands were quantified by whole band analysis using a Bioimage electrophoresis analyzer (Millipore Corp.).
‡ Molar ratios ezrin/actin ($\times 10^{-4}$). The amount of ezrin present in column elutions was calculated as a fraction of a known standard (unfractionated lysate; 7.7 pmol/10^6 cells); and the molar ratio determined by the moles ezrin bound/mole actin Sepharose-4B, where the concentration of actin conjugated to Sepharose-4B is 5 μM.
§ ND = not detectable.

creases with cell motility (see Fig. 5). We cannot detect ezrin p55 when lysates are prepared in the presence of EGTA (Fig. 2, lane 2), nor in any of our 1 M KCl elutions from α- or β-actin affinity columns (Fig. 2, lanes 2–13). Ezrin-β-actin interactions can be sustained in the presence of 0.2 mM CaCl₂ when either of the two calpain I-specific inhibitors, E64 (L-trans-epoxysuccinyl-leucylamido[4-guanidino]butane) or calpain inhibitor I (N-Ac- [leucyl]₂-norleucinal) are included in the extraction and affinity fractionation buffers (Barrett et al., 1982; Tusjinaka et al., 1988) (Fig. 2, lane 7; Table I).

Cytochalasin D Inhibits Association of Ezrin with β-actin Sepharose-4B

To test whether ezrin binding to β-actin occurs via the ends or along the sides of the β-actin filament, we next asked if cytochalasin D treatment of phalloidin-stabilized β-actin filament matrices could prevent ezrin's association. When ezrin-containing Eₘ are percolated over β-actin–Sepharose-4B columns in the presence of 2 μM cytochalasin D, ezrin binding to β-actin is completely blocked (n = 4) (Fig. 2, lane 13). The CD inhibition of ezrin binding is reversible, since ezrin and bABP binding to β-actin Sepharose-4B is restored when CD is washed from the column. This indicates that the effect is not due to CD-induced depolymerization of the actin filaments. Electron microscopy of negatively stained phalloidin-stabilized actin filaments treated with 2 μM CD also confirms that cytochalasin D is not depolymerizing actin from the affinity columns (Shuster, C. B., unpublished observations), but does not rule out the possiblity that another β-actin-specific binding protein is responsible for mediating the CD-sensitive β-actin capping/ezrin association (see below) (Figs. 8 and 9).

Association of Ezrin and β-actin In Vivo: Co-precipitation Using Covalent Cross-linkers

To reveal whether an ezrin-β-actin complex could be isolated from living cells, co-immune precipitation was employed. To stabilize ezrin-β-actin interactions prior to cell lysis, biosynthetically labeled cells were treated with DSP as described (see Materials and Methods). Fluorographic analysis of immune precipitates electrophoresed on 7.5% polyacrylamide gels reveals that β-actin and ezrin can be coprecipitated using anti-actin IgG (Fig. 3, lane 1). Ezrin cannot, on the other hand, be co-precipitated from the DSP cross-linked, α-actin-containing stress fiber fraction (Eₛ)

(Fig. 3, lane 2). In addition to the ezrin and β-actin present in the co-precipitates, there is one prominent band at 45 kD, and another at approximately 73 kD (Fig. 3, lane 1, asterisk), which is most likely p73 seen in the 1.0 M releasate from the β-actin column (Fig. 1, lane 4). The 45-kD polypeptide is
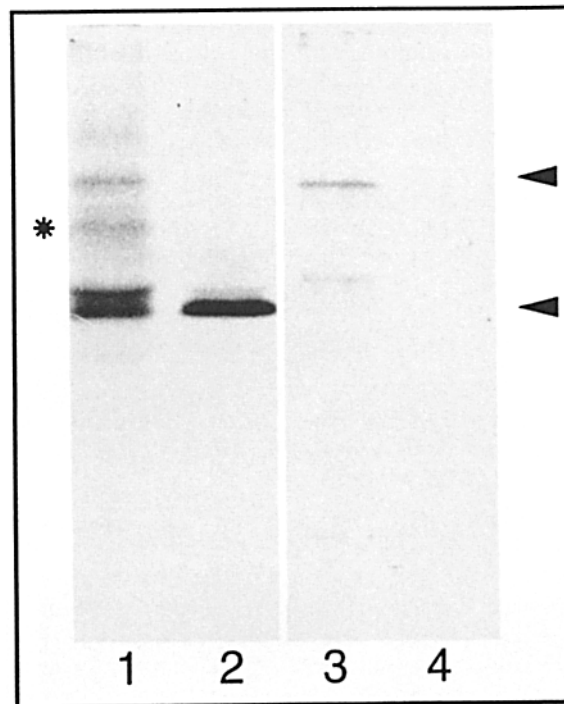

Figure 3. Co-precipitation of ezrin and β-actin from DSP crosslinked cytoplasm. Retinal pericytes were labeled with 85 μCi/ml [³⁵S]methionine/[³⁵S]cysteine for 10 h. Cells were washed three times with PBS prior to treatment of 0.25 mM Dithiobis[succinimidylpropionate] (DSP) in PBS/0.005% digitonin for 10 min. Lysis and immunoprecipitation were performed on Triton-soluble (lanes 1 and 3) and SDS-soluble (lanes 2 and 4) fractions as described (Yost and Herman, 1990). Precipitates were washed, solubilized in SDS-PAGE sample buffer. Samples were resolved on 7.5% SDS-PAGE, and processed for fluorography. (Top arrow) Ezrin; (Bottom arrow) actin; (Asterisk) p73 (lane 1). (Lanes 1 and 2) Anti-actin immunoprecipitates from Triton-soluble (lane 1) and SDS-soluble (lane 2) lysates. (Lanes 3 and 4) Anti-ezrin immunoprecipitates from Triton-soluble (lane 3) and SDS-soluble (lane 4) lysates.

an electrophoretic variant of actin (confirmed by Western blotting), and the 73 kD species is novel and under study.

Ezrin and β-Actin are Co-localized within Leading Lamellae and Rearward Protrusions

Because ezrin associates specifically with β-, but not α-actin filaments in vitro, we examined whether the proteins are co-localized within cells. We turned to our "wound healing" model, where we have already demonstrated that β-actin and its encoding mRNA are rapidly recruited and retained within the advancing protrusions of crawling cells, which migrate in response to monolayer injury in vitro (Hoock et al., 1991). Using affinity-selected anti-β-actin IgG and monoclonal anti-ezrin IgG, we can simultaneously localize ezrin and β-actin within the distal reaches of advancing protrusions and in membrane veils undergoing rapid ruffling (Fig. 4). Broad fan lamellae that slowly extend forward as well as rearward regions that are released from contact inhibition are also β-actin and ezrin-rich (data not shown). Bright foci of β-actin and ezrin (1.32 ± 0.4 μm^2) can also be seen within the ventral aspects of forward protrusions behind the leading edge, and in apical projections that move centripetally toward the nucleus (Fig. 4, *A* and *B*). These co-localization patterns are independent of the nonmuscle cell type studied, i.e., in each case, ezrin and β-actin are exclusively seen within the membrane–cytoskeletal interface and are particularly prevalent within domains that engage in cytoplasmic remodelling, either during cell locomotion or protrusion formation.

Ezrin Proteolysis Is Elevated in Motile Cells

Based on results of isoactin affinity fractionation experiments where Ca^{2+}-activated calpain I modulates ezrin–β-

actin interactions, we wished to determine whether such a mechanism might be in place in crawling cells. To these ends, extracts were derived from populations of stationary endothelial cells and those undergoing a uniform, migratory response to injury. Confluent monolayers of endothelial cells were injured with a rake that creates concentrically uniform, denuded zones that are 400–600 μm in width (Herman, 1993c). Following injury and during the recovery (motile) phase, cultures were lysed and probed for the presence of intact and ezrin p55 with polyclonal anti-ezrin IgG. Western blotting reveals the accumulation of ezrin p55 by 30 min after injury, which persists through the motile, wound-healing phase (Fig. 5). During post-injury motility, ezrin p55 levels are 14–18-fold greater than at the time of injury.

Cytosolic-free Calcium Is Transiently Elevated within Ezrin and β-Actin–enriched Cytoplasmic Domains

Results from the isoactin affinity fractionation, co-immune precipitation and antibody localization studies indicate that ezrin and β-actin interact in a calcium-sensitive fashion. Could local elevations in free calcium be found in ezrin–actin-rich cytoplasmic domains during the migratory response to injury in vitro? Using fluo-3 and confocal microscopy qualitative assessments of free calcium transients were made in endothelial cells recovering from injury in vitro. Image analysis of fluo-3 fluorescence across the injured monolayer reveals that cells crawling at the wound edge possess a threefold greater level of free calcium than those cells within the resting monolayer, which are 7.5–8 cell diameters from the injury site (Fig. 6). Within forward protrusions, bursts of fluo-3 fluorescence emerge and then disappear as moving cytoplasm advances along the wound edge. Bright perinuclear and organellar fluorescence can also be seen.
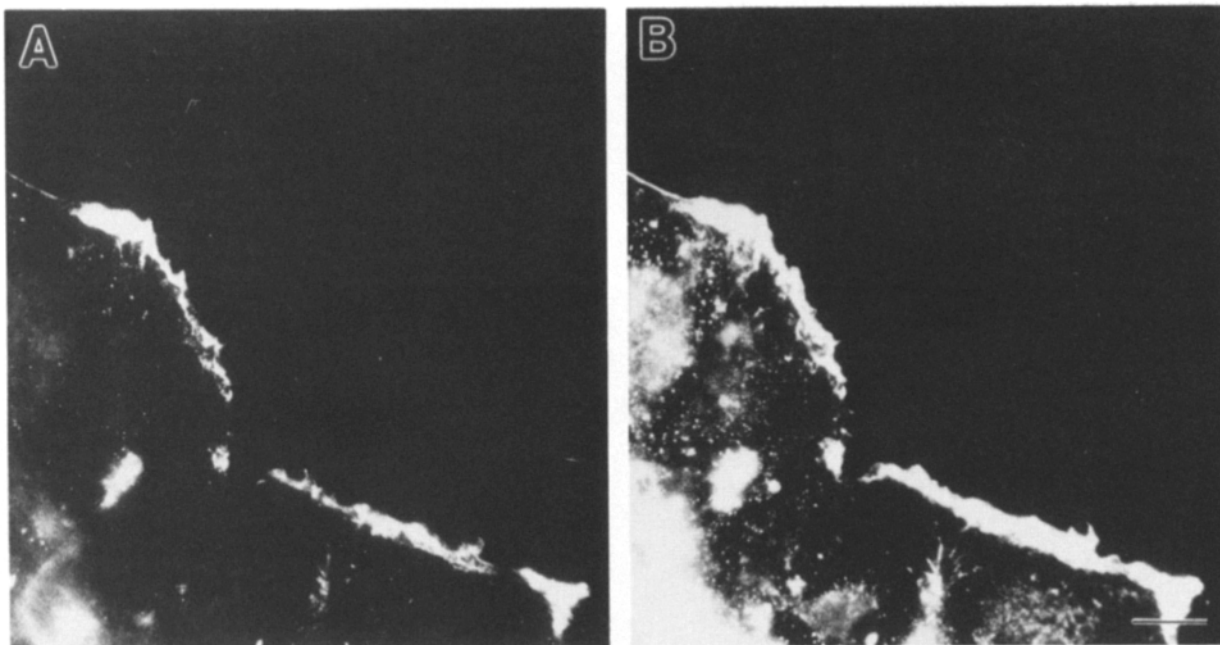

Figure 4. β-actin and ezrin are co-localized in leading lamellae. Bovine endothelial cells were plated at confluence onto glass coverslips. Monolayers were injured as described and allowed to recover for 60 min at 37°C prior to fixation and permeabilization (Hoock et al., 1991). Cells were stained simultaneously with affinity-selected anti-β-actin IgG (detected with rhodamine-labeled goat anti-rabbit IgG) (*A*) and monoclonal anti-ezrin IgG (detected with fluorescein-labeled goat anti-mouse IgG) (*B*). Bar, 10 μm.
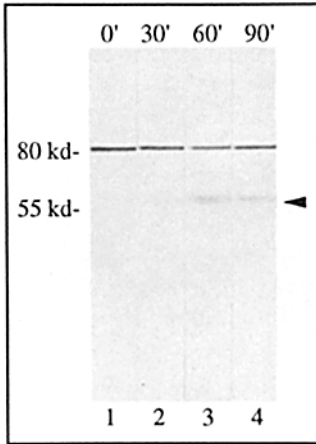
Figure 5. Ezrin proteolysis is elevated in motile cells. Bovine endothelial cells, which are plated at confluence, are injured as described (Herman, 1993c). Cells are allowed to recover from 0–90 min after injury. Lysates are then prepared from crawling or control cells. Lanes *1-4*, Western blot, anti–ezrin IgG. Arrow indicates the emergence of ezrin p55, the calpain I–generated proteolytic breakdown product. (Lane *1*) Control, no motility (0 time). (Lane *2*) 30 min after injury. (Lane *3*) 60 min after injury. (Lane *4*) 90 min after injury.

Within live cell cultures, 45% ± 2.18 of fluo-3 fluorescence is observed as discrete focal domains occupying 2.7 ± 2 μm^2. In other cells 12% ± 2.33 of the fluo-3 fluorescence is diffuse, extending back from the wound edge, enveloping the entire cortex and occupying roughly 67 ± 28.8 μm^2. In 9% of cells bordering the wound edge, the entire cytoplasm is filled with a low level of fluo-3 fluorescence.

Following confocal imaging of fluo-3 fluorescence in live cell cultures, we mapped regions of overlap between free calcium, ezrin and β-actin by fixing the identical cultures and preparing them for double antibody staining. Co-localization reveals that fluo-3 fluorescence maps to within 70% ± 2.5 of the ezrin- and β-actin–rich domains (Fig. 6). Quantitative analysis reveals that ezrin is localized within 2.6 ± 1.8 μm of the leading edge ($n = 38$), and is found exclusively in the cortex (Fig. 6). β-actin is present within the ezrin "shell," extending only 1.57 ± 0.77 μm from the leading edge ($n = 38$) (Fig. 6). Fluo-3 fluorescence envelops the entire ezrin–β-actin–rich zone, leaving a statistically significant area of overlap of ~1.35 μm. A t-test reveals that non-overlap between ezrin and free calcium is not statistically significant ($P = 0.427$).

Pericyte Ezrin Does Not Directly Bind β-Actin Filaments In Vitro

Co-sedimentation and Co-immunoprecipitation. To address whether ezrin binds β-actin filaments directly or through other components, we mixed homogeneous preparations of ezrin with α- or β-actin filaments in vitro. 0.5 μM hydroxylapatite- and DE-52–purified pericyte ezrin (Fig. 7)
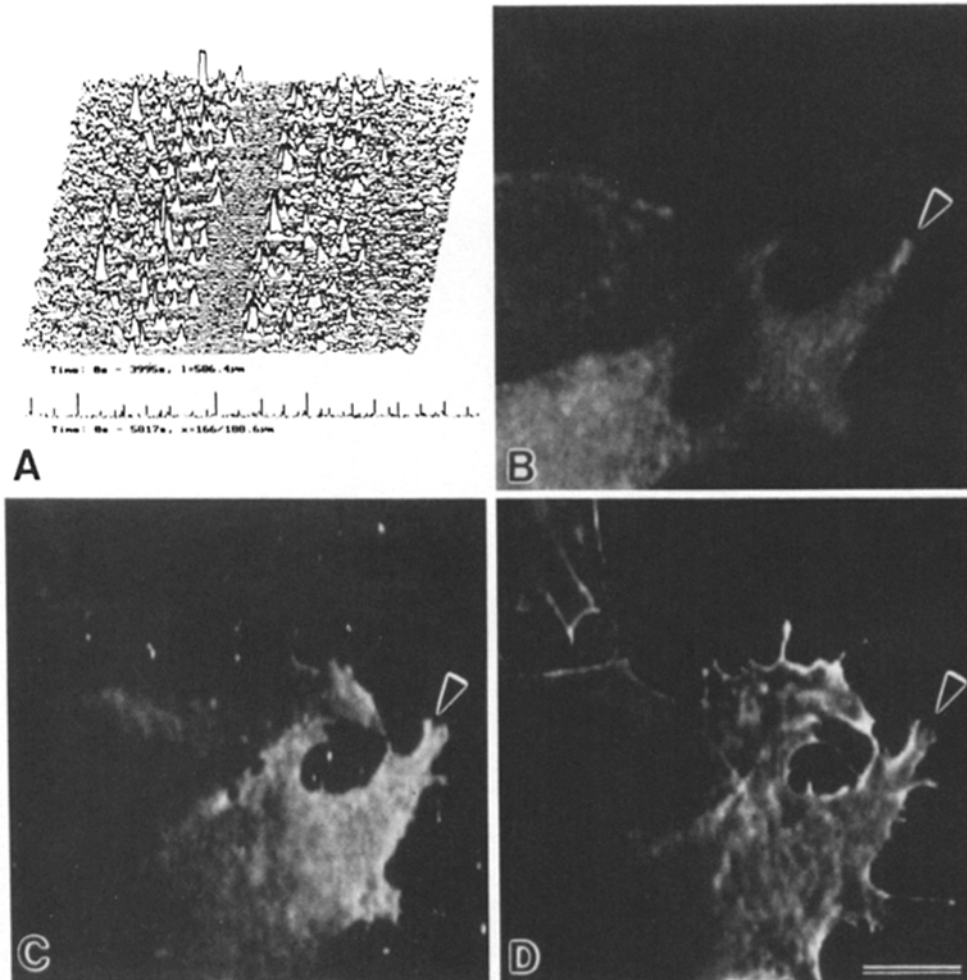

Figure 6. Simultaneous mapping of free calcium in ezrin–β-actin–rich cytoplasmic domains. Bovine endothelial cells were plated at confluence and injured in the presence of 5 μM Fluo-3. Cells were allowed to recover for 25 min at 37°C, prior to mounting on a warmed chamber slide. Fluo-3 fluorescence was monitored by confocal microscopy, and qualitative differences in free calcium levels are shown in *A* as a histogram of fluo-3 fluorescence observed in cells bordering both sides of the wound edge, with each peak representing the fluorescence of a single cell along its x-axis. Cortical-free Ca^{2+} in cells bordering the wound edge are shown in *B*. Following image capture, cells were fixed and processed for ezrin (*C*) and β-actin (*D*) localization. Bar, 10 μm.
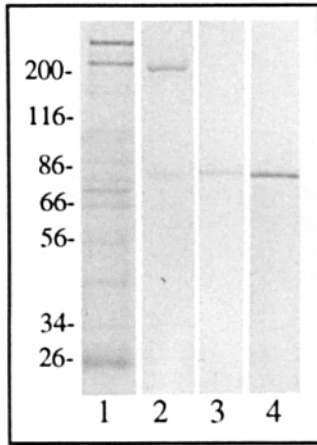
844

Figure 7. Purification of pericyte ezrin. (Lanes *1–3*) Coomassie brilliant blue R-250. (Lane *4*) Western blot, anti-ezrin IgG. E_m extracted from subconfluent cultures of bovine retinal pericytes (lane *1*) was chromatographed over hydroxylapatite as described in Materials and Methods. Ezrin-enriched fractions were pooled (lane *2*) and re-chromatographed over DEAE cellulose. The 0.1 M NaCl fraction eluted from the column contains purified ezrin (lane *3*) as confirmed by Western blotting using rabbit anti–ezrin IgG (lane *4*).

were mixed together with either 0.5 μM α- or β-actin under physiological ionic conditions and over a pH range (7.0–8.5) prior to sedimentation of actin filaments at 110,000 g. Taking into account our earlier isoactin affinity fractionation data indicating that ezrin putatively binds to the barbed end of the β-actin filament (Fig. 2, lane *13*), affinity-purified pericyte ezrin (8–16 nM) was combined at ratios that were 5–10-fold greater than the estimated number of free isoactin filament ends. Examination of soluble and pellet fractions reveals that ezrin cannot be co-sedimented with either α- or β-actin filaments under any condition ($n = 12$) (Fig. 8). Further, as we have demonstrated that ezrin present within lamellar lysates associates with β-actin–Sepharose 4B, it can also be shown that ezrin sediments with β-actin when this isoactin is added to the lamellar lysate (Fig. 8). Increasing actin concentrations or altering the incubation temperature/time yielded identical results (data not shown). As an alternative, perhaps more sensitive means of assessing these protein–protein interactions, we again employed our actin antibodies to co-precipitate ezrin/isoactin complexes from these purified protein mixtures. Western blotting of actin immunoprecipitates indicates that ezrin cannot be detected in the immunoprecipi-

tates of either α- or β-actin filaments pre-incubated in the presence of ezrin (data not shown).

Isoactin Affinity Fractionation. As a final assessment of whether ezrin binding to β actin is direct, we applied purified ezrin to the isoactin Sepharose-4B columns under experimental conditions identical to those we had initially established as being supportive for the β-actin–ezrin interactions described in Fig. 2. Western blotting of the unbound fraction as well as the material released with 1.0 M NaCl indicates that ezrin does not directly bind to either α-or β-actin affinity columns, while control experiments using E_m containing ezrin reaffirms our earlier results, which suggest that ezrin binding to β-, but not α-actin is specific, indirect, and most likely to be mediated through other accessory protein(s) (Fig. 9).

Discussion

We have been able to conclusively demonstrate that ezrin, one member of the recently discovered ERM family of putative tumor suppressor proteins (Tsukita et al., 1993), interacts specifically with β-, but not α-actin filaments. Further, this association is sensitive to calcium, through the action of calpain I. The in vitro association between β-actin and ezrin is not only consistent with their co-localization within distal reaches of forward protrusions, but is also supported by the transient increase of cytosolic free calcium within the ezrin–β-actin–enriched cell cortex. In addition, we find that when cells undergo a migratory response to injury and position both ezrin and β-actin in leading lamellae, ezrin proteolysis is elevated. Co-immune precipitation of ezrin from E_m-derived lysates using actin antibodies confirms both the morphological and biochemical observations and suggests that the two proteins are, indeed, interactive in vivo. However, co-sedimentation, co-precipitation, and isoactin affinity fractionation experiments reveal that a direct interaction between ezrin and β-actin is unlikely, since homogenous, native preparations of ezrin fail to bind either isoactin under any experimental condition tested. The results of these studies suggest that ezrin most likely interacts with a β-actin–
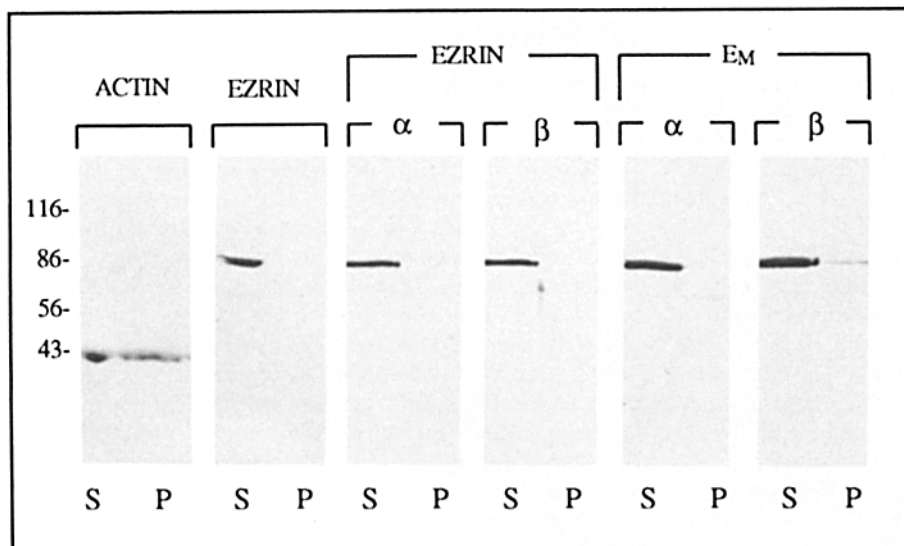

Figure 8. Co-sedimentation analysis of ezrin–actin interactions. Ezrin was incubated alone or in the presence of filamentous (0.5 μM, α or β) actin prior to pelleting by centrifugation (*middle, purified Ezrin*). Alternatively, the identical experiment was performed using lamellar extracts (*right, E_m*). Supernatant (*S*) and pellet (*P*) fractions were analyzed by Western blotting with anti-ezrin IgG. Actin polymerized and pelleted in the absence of ezrin is shown (*left*, Coomassie brilliant blue R-250 staining). Molecular weight markers in kD are shown). The addition of ezrin does not influence the amount of actin sedimented.
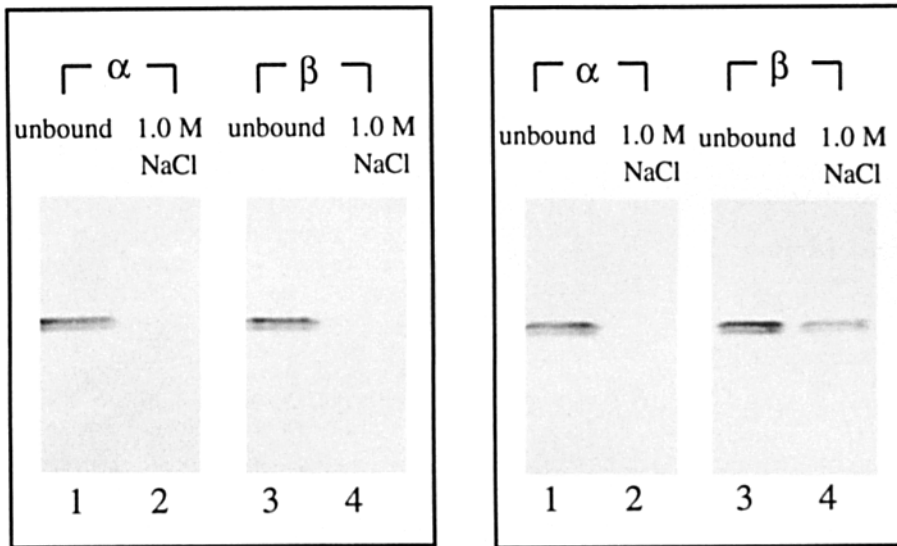
Figure 9. Affinity fractionation of purified pericyte ezrin. Pericyte ezrin (*left panel*) was incubated with α- or β-actin Sepharose-4B under conditions described for affinity fractionation of E_m-derived lysates (Figs. 1, 2 and *right panel*). For controls, E_m was percolated over α- or β-actin Sepharose-4B following its pre-absorbtion over α-actin Sepharose-4B (*right panel*). Columns were washed and eluted as described, and the protein that remained unbound, or that which was released with 1.0 M NaCl was probed by Western blotting with anti–ezrin IgG (lanes *1–4, both panels*). (Lane *1*) Unbound fraction from α-actin Sepharose-4B. (Lane 2) 1.0 NaCl elution from α-actin Sepharose-4B. (Lane 3) Unbound fraction from β-actin Sepharose-4B. (Lane 4) 1.0 NaCl elution from β-actin Sepharose-4B.

specific binding protein, and that proteolytic modification of ezrin dissociates it from the β-actin filament complex.

Ezrin Association with F-Actin Isoform Specificity

Binding of ezrin of F-actin is currently controversial. Originally, ezrin was not considered to be an actin-binding protein, as it did not associate with muscle actin in vitro (Bretscher, 1983, 1991). More recently, it has been reported that ezrin does contain an actin-binding domain at its COOH terminus. Independent expression of this decapeptide demonstrates that it possesses a strong affinity for both skeletal muscle and cytoplasmic actin (Turenen et al., 1994). Our data suggest that the actin-binding activity of the expressed COOH-terminal domain may not reflect the behavior of the intact, native ezrin molecule, since we could not detect any binding of skeletal muscle actin, and no direct association with β-actin.

In our hands, only ezrin contained with cell lysates (derived from moving cytoplasm) associates with β-, but not α-actin filaments in vitro (Fig. 2, 8, and 9). Purified, intact ezrin does not bind to either isoactin affinity columns or native filaments when the identical experiments are performed with purified molecules (Fig. 9). Co-sedimentation and -immunoprecipitation experiments designed to detect direct binding between affinity-purified ezrin and β-actin filaments fail to reconstitute this interaction (Fig. 8). This suggests that one or more polypeptides present in the lamellar lysates, which do not bind α-actin, potentiates ezrin binding to the β-actin filament. There are five possible polypeptides eluting from β-actin affinity columns along with ezrin (Fig. 1) that might be responsible for such an interaction. Co-precipitations of ezrin and β-actin (from labeled cell lysates) contain a polypeptide of ∼73 kD (Fig. 3), which does not bind to α-actin and is also present in the β-actin column releasates (Fig. 1). It is possible that ezrin binds p73, which in turn caps the barbed end of the β-actin filament. That cytochalasin D

blocks ezrin binding to β-actin when p73 is present suggests that this is, indeed, the case.

Morphological studies examining actin interactions with the plasma membrane have reported that actin is joined to the plasma membrane at its ends and along its sides (Luna and Hitt, 1993). End-on associations of actin filaments with the plasma membrane have been described in several model systems, including the intestinal epithelial cell brush border, where bundled arrays of actin filaments terminate at the plasma membrane via their barbed ends (reviewed by Bretscher, 1991). The pointed ends of actin filaments have also been shown to interact with the plasma membrane in the advancing front of nerve growth cones (Lewis and Bridgman, 1992). Lateral associations of actin filaments with the plasma membrane have also been documented. In *Dictyostelium*, actin filament–membrane interactions are mediated through an integral membrane protein, ponticulin (Wuesteuhube and Luna, 1987). Ponticulin organizes actin by binding the sides of filaments, but this binding is not isoactin-specific. Our own immunoelectron microscopic examination of β-actin filament organization in leading lamellae and other forward protrusions indicates that short stretches of β-actin filaments (7–10 molecules in length) terminate at the plasma membrane. From these anti–β-actin IgG-decorated nuclei, undecorated γ-actin–containing filaments could extend (Shujath, J., and I. M. Herman, unpublished observations). Our biochemical data, which indicates that cytochalasin D blocks the interaction of ezrin/p73 with β-actin in vitro (Fig. 2), suggests that the ezrin/p73 complex associates at or in close approximation to the fast growing end of the β-actin nucleus, at the plasma membrane (Figs. 2 and 3). Indeed, studies using fluorescent derivatives of actin in permeabilized cell models suggest that a regulated, barbed-end capping activity exists at the tips of lamellipodia (Symons and Mitchison, 1991). Collectively, these data point to a possible role for ezrin in tethering a β-actin filament capping complex at the plasma membrane. However,

more work is required before the details of these putative events are understood.

Ca²⁺-activated Proteolysis Regulates Ezrin–β-Actin Interactions

Our results performing isoactin affinity fractionation in the presence of calcium and/or calpain-specific inhibitors reveal that ezrin undergoes a calpain I–mediated cleavage, and this abolishes its ability to associate β-actin in vitro (Fig. 2). And in vivo, there is an accumulation of the ezrin p55 proteolytic breakdown product as cells polarize and crawl in response to monolayer injury. This is not the first report indicating that modulation of protein–protein interactions can occur by calcium-activated proteolysis. During platelet activation, local elevations of intracellular calcium induce an autolytic cleavage of calpain I, activating the protease (Saido, 1992). In its activated state, calpain I is localized at the plasma membrane, where it acts on filamin and fodrin (Fox et al., 1985; Saido et al., 1993). Also, activation of erythrocyte calpain I (with ionophores) results in protein 4.1 and spectrin degradation (Hayashi et al., 1991). More pertinent to our findings are indications that calpain I mediates the limited proteolysis of parietal cell ezrin both in vitro and in vivo. In vivo, calpain I–mediated degradation of parietal cell ezrin results in the inhibition of proton secretion (Yao et al., 1993). Based on these findings, we postulate that β-actin–ezrin interactions may be regulated via a calpain-mediated cleavage. The calpain-mediator turnover of ezrin, as well as other cytoskeletal components, may facilitate the remodelling of the actin cytoskeleton, and allow for new monomer addition at the plasma membrane within forward protrusions. Our observations that cytosolic-free calcium is transiently elevated in forward protrusions and that ezrin proteolysis is also elevated in motile cells lends credence to this notion (c.f. Figs. 5 and 6).

It should be pointed out that elevations in free calcium have been carefully monitored in single crawling cells using ratio imaging analysis (Hahn et al., 1992; Brundage et al., 1991). Results reveal that the highest free calcium concentration is present in the trailing, contracting portion of the cell (Hahn et al., 1992; Brundage et al., 1991). Based on this work, it has been proposed that elevated free calcium leads to myosin II–mediated contraction of the posterior cytoplasm, therein providing a protrusive force propelling cytoplasm and actin monomers forward for polymerization at the leading lamellae (Gough and Taylor, 1993). However, computer-assisted analysis of endothelial motility following injury reveals a deliberate, sheet-like migration of the monolayer where pseudopodial and lamellar extension occur in the absence of any significant rearward contraction (Askey and Herman, 1988; Herman, 1993b). All of these observations are consistent with our present work, which reveals that calcium is transiently elevated within leading lamellae in the majority of cells surveyed along the wound edge (Fig. 6). This temporal and spatial rise and fall of free calcium in discrete cytoplasmic domains may dictate where calpain I could cleave ezrin and release β-actin for barbed end assembly. It will be important to reveal whether p73 is not capable of binding ezrin after Ca²⁺/calpain-mediated cleavage or it p73 dissociates from the β-actin filament with ezrin p55. Current studies are focused on these open questions.

References

Algrain, M., O. Turunen, A. Vaheri, D. Louvard, and M. Arpin. 1993. Ezrin contains cytoskeleton and membrane binding domains accounting for its proposed role as a membrane-cytoskeletal linker. *J. Cell Biol.* 120:129–139.

Askey, D. B., and I. M. Herman. 1988. Computer-assisted analysis of the vascular endothelial motile response to injury. *Comp. Biomed. Res.* 21: 551–561.

Barrett, A. J., A. A. Kembhavi, M. A. Brown, H. Kirschke, C. G. Knight, M. Tamai, and K. Hanada. 1982. L-*trans*-Epoxysuccinyl-Leucylamido(4-guanidino)butane (E-64) and its analogues as inhibitors of cysteine proteinases including cathepsins B, H and L. *Biochem. J.* 201:189–198.

Bennett, V. 1985. The membrane skeleton of human erythrocytes and its implications for more complex cells. *Annu. Rev. Biochem.* 54:273–304.

Birgbauer, E., and F. Solomon. 1989. A marginal band-associated protein has properties of both microtubule- and microfilament-associated proteins. *J. Cell Biol.* 109:1609–1620.

Bretscher, A. 1983. Purification of an 80,000-dalton protein that is a component of the isolated microvillus cytoskeleton and its localization in cultured cells. *J. Cell Biol.* 97:425–432.

Bretscher, A. 1985. Purification of the intestinal microvillus cytoskeletal proteins villin, fimbrin, and ezrin. *Methods Enzymol.* 134:24–37.

Bretscher, A. 1989. Rapid phosphorylation of ezrin and spectrin accompany morphological changes induced in A431 cells by epidermal growth factor. *J. Cell Biol.* 108:921–930.

Bretscher, A. 1991. Microfilament structure and function in the cortical cytoskeleton. *Annu. Rev. Cell Biol.* 7:337–374.

Brundage, K. A., K. E. Fogarty, R. A. Tuft, and F. S. Fay. 1991. Calcium gradients underlying polarization and chemotaxis of eosinophils. *Science (Wash. DC).* 254:703–706.

Cohen, S. A., T. L. Tarvin, B. A. Bidlingmeyer, and G. E. Tarr. 1984. Analysis of amino acids using pre-column derivitization phenylisothiocyanate. *Am. Lab.* 48.

DeNofrio, D., T. C. Hoock, and I. M. Herman. 1989. Functional sorting of actin isoforms in microvascular pericytes. *J. Cell Biol.* 109:191–202.

Fox, E. B., C. C. Reynolds, J. S. Morrow, and D. R. Phillips. 1985. Spectrin is associated with membrane-bound actin filaments in platelets and is hydrolyzed by the Ca⁺⁺-dependent protease during platelet activation. *Blood.* 69:537–545.

Gough, A. H., and D. L. Taylor. 1993. Fluorescence anisotropy imaging microscopy maps calmodulin binding during cellular contraction and locomotion. *J. Cell Biol.* 121:1095–1107.

Gould, K. L., A. Bretscher, F. S. Esch, and T. Hunter. 1989. cDNA cloning and sequencing of the protein-tyrosine kinase substrate, ezrin, reveals homology to band 4.1. *EMBO (Eur. Mol. Biol. Organ.) J.* 8:4133–4142.

Hahn, K., R. DeBiasio, and D. L. Taylor. 1992. Patterns of elevated free calcium and calmodulin activation in living cells. *Nature (Lond.).* 359:736–738.

Hayashi, M., M. Inomata, Y. Saito, H. Ito, and S. Kawashima. 1991. Activation of intracellular calcium-activated neutral proteinase in erythrocytes and its inhibition by exogenously added inhibitors. *Biochem. Biophys. Acta.* 1904:249–256.

Herman, I. M. 1988. Developing probes and methods for morphological and biochemical analyses of cytoskeletal elements in vascular cells. *CRC Crit. Rev. Anat. Sci.* 1:133–148.

Herman, I. M. 1993a. Actin isoforms. *Curr. Opin. Cell Biol.* 5:48–55.

Herman, I. M. 1993b. Microvascular pericytes in development and disease. *In* The Blood-Brain Barrier. Raven Press, LTD, New York.

Herman, I. M. 1993c. Molecular mechanisms regulating the vascular endothelial cell motile response to injury. *J. Cardiovasc. Pharm.* 22(suppl. 4): 225–236.

Herman, I.M., and T. D. Pollard. 1979. Comparison of purified anti-actin and fluorescent heavy meromyosin staining patterns in dividing cells. *J. Cell Biol.* 80:509–520.

Herman, I. M., and P. A. D'Amore. 1985. Microvascular pericytes contain muscle and nonmuscle actins. *J. Cell Biol.* 101:43–52.

Hill, M. A., and P. Gunning. 1993. Beta and gamma actin mRNAs are differentially located with myoblasts. *J. Cell Biol.* 122:825–832.

Hill, M. A., L. Schedlich, and P. Gunning. 1994. Serum-induced signal transduction determines the peripheral localization of β actin mRNA within the cell. *J. Cell Biol.* 126:1221–1230.

Hoock, T. C., P. M. Newcomb, and I. M. Herman. 1991. β actin and its mRNA are localized at the plasma membrane and the regions of moving cytoplasm

during the cellular response to injury. *J. Cell Biol.* 112:653–664.

Kislauskis, E. H., Z. Li, R. H. Singer, and K. L. Taneja. 1993. Isoform-specific 3' untranslated sequences sort alpha cardiac and beta cytoplasmic actin mRNAs to different cytoplasmic compartments. *J. Cell Biol.* 123:165–172.

Kislauskis, E. H., X. Zhu, and R. H. Singer. 1994. Sequences responsible for intracellular localization of β actin messenger RNA also affect cell phenotype. *J. Cell Biol.* 127:441–451.

Laskey, R. A., and A. D. Mills. 1975. Quantitative film detection of ³H and ¹⁴C in polyacrylamide gels by fluorography. *Eur. J. Biochem.* 45:335–341.

Leavitt, J., and G. Bushar. 1982. Variation in expression of mutant β Actin accompanying incremental increases inhuman fibroblast tumorigencity. *Cell.* 28:259–268.

Leavitt, J., S.-Y. Ng. U. Aebi, M. Varma, G. Latter, S. Burbeck, L. Kedes, and P. Gunning. 1987. Expression of transfected mutant β-actin genes: alteration of cell morphology and evidence for autoregulation of actin pools. *Mol. Cell. Biol.* 7:2457–2466.

Lenk, R., L. Ransom, Y. Kaufman, and S. Penman. 1977. A cytoskeletal structure with associated polyribosomes obtained from HeLa cells. *Cell.* 10: 67–78.

Lewis, A. K., and P. C. Bridgman. 1992. Nerve growth cone lamellipodia contain two populations of actin filaments that differ in organization and polarity. *J. Cell Biol.* 119:1219–1243.

Lubit, B. W., and J. H. Schwartz. 1980. An antiactin antibody that distinguishes between cytoplasmic and skeletal muscle actins. *J. Cell Biol.* 86:891–897.

Luna, E. and A. L. Hitt. 1992. Cytoskeletal-plasma membrane interactions. *Science (Wash. DC).* 258:955–964.

Ohmori, H., S. Toyama, and S. Toyama. 1992. Direct proof that the primary site of action of cytochalasin on cell motility processes is actin. *J. Cell Biol.* 116:933–941.

Otey, C. A., M. H. Kalnoski, and J. C. Bulinski. 1988. Immunolocalization of muscle and nonmuscle isoforms of actin in myogenic cells and adult skeletal muscle. *Cell. Motil. & Cytoskel.* 9:337–348.

Pinder, J. C., and W. B. Gratzer. 1983. Structural and dynamic states of actin in the erythrocyte. *J. Cell Biol.* 96:768–775.

Puszkin, S., J. Maimon, and E. Puzkin. 1978. Erythrocyte actin and spectrin: interactions with muscle contractile and regulatory proteins. *Biochem. Biophys. Acta.* 513:205–220.

Rubenstein, P. 1981. Differential behavior of gizzard isoactins. *Arch. Biochem. Biophys.* 210:598–608.

Rubenstein, P. 1990. The functional importance of multiple actin isoforms. *Bioessays.* 12:309–315.

Saido, T. C., S. Nagao, M. Shiramine, M. Tsukaguchi. H. Sorimachi, H. Murofushi, T. Tsuchiya, H. Ito, and K. Suzuki. 1992. Autolytic transition of μ-calpain upon activation as resolved by antibodies distinguished between the pre- and post-autolysis forms. *J. Biochem.* 111:81–86.

Saido, T. C., H. Suzuki, H. Yamazaki, K. Tanoue, and K. Suzuki. 1993. In situ capture of μ-calpain activation in platelets. *J. Biol. Chem.* 268:7422–7426.

Schevzov, G., C. Lloyd, and P. Gunning. 1992. High level expression of transfected beta and gamma actin genes differentially impacts myoblast cytoarchitecture. *J. Cell Biol.* 117:775–785.

Spudich, J. A., and S. Watt. 1971. The regulation of rabbit skeletal muscle contraction. I. Biochemical studies of the interaction of the troponin-tropomyosin complex with actin and the proteolytic fragments of myosin. *J. Biol. Chem.* 246:4866–4880.

Sundell, C. L., and R. H. Singer. 1990. Actin mRNA localizes in the absence of protein synthesis. *J. Cell Biol.* 111:2397–2403.

Sundell, C. L., and R. H. Singer. 1991. Requirement of microfilaments in sorting of actin mRNA. *Science (Wash. DC).* 253:1275–1277.

Symons, M. H., and T. J. Mitchison. 1991. Control of actin polymerization in live and permeabilized fibroblasts. *J. Cell Biol.* 114:503–513.

Tsujinaka, T., Y. Kajiwara, J. Kambayashi, M. Sakon, N. Higuchi, T. Tanaka, and T. Mori. 1988. Synthesis of a new cell penetrating calpain inhibitor (Calpeptin). *Biochem. Biophys. Res. Commun.* 153:1201–1208.

Tsukita, S., M. Itoh, A. Nagafuchi, S. Yonemura, and S. Tsukita. 1993. Submembranous junctional plaque proteins include potential tumor suppressor molecules. *J. Cell Biol.* 123:1049–1053.

Turenen, O., T. Wahlström, and A. Vaheri. 1994. Ezrin has a COOH-terminal actin-binding site that is conserved in the ezrin protein family. *J. Cell Biol.* 126:1445–1453.

Westeuhube, L. J., and E. Luna. 1987. F-actin binds to the cytoplasmic surface of ponticulin, a 17 Kd integral glycoprotein from *Dictyostelium discoideum.* *J. Cell Biol.* 105:1741–1751.

Yao, X., A. Thibodeau, and J. G. Forte. 1993. Ezrin-calpain I interactions in gastric parietal cells. *Am. J. Physiol.* 265:C36–C46.

Yost, J. C., and I. M. Herman. 1990. Substratum-induced stress fiber assembly in vascular endothelial cells during spreading in vitro. *J. Cell Sci.* 95: 507–520.